Finite Volume Evolution Galerkin (FVEG) Methods for Three-Dimensional Wave Equation System

M. Lukáčová-Medviďová[1], G. Warnecke[2] and Y. Zahaykah[2,3]

Abstract

The subject of the paper is the derivation of finite volume evolution Galerkin schemes for the three-dimensional wave equation system. The aim is to construct methods which take into account all of the infinitely many directions of propagation of bicharacteristics. The idea is to evolve the initial function using the characteristic cone and then to project onto a finite element space. Numerical experiments are presented to demonstrate the accuracy and the multidimensional behaviour of the solutions. Moreover, we construct further new EG schemes by neglecting the so-called source term, i.e. we mimic Kirchhoff's formula. The numerical test shows that such schemes are more accurate and some of them are of second order.

Key words: hyperbolic systems, wave equation, evolution Galerkin schemes, recovery stage, finite volume.

1 Introduction

Evolution Galerkin methods, EG-methods, were proposed to approximate evolutionary problems for first-order hyperbolic systems. They belong to the class of genuinely multidimensional schemes. The main aim is to have a scheme which takes into account all infinitely many directions of wave propagation. We refer the reader to [1], [4], [5], [8], [12], [23] for other recent multidimensional schemes.

The EG-schemes were introduced by Morton *et al.* for scalar problems and one-dimensional systems, see [10, 11]. Actually the research of Bill Morton and his collaborators was motivated by the pioneering work of Butler [3] and related works of Prasad [25, 26]. It was Stella Ostkamp [24] who firstly generalized these schemes to approximate the solution of the wave equation system as well as the Euler equations of gas dynamics in two space dimensions. In [13] Lukáčová, Morton and Warnecke derived for the linear two-dimensional wave equation system new EG-schemes with better accuracy and stability. Further, in [29] the approximate evolution operator of the wave equation system in three space dimensions as well as other two-dimensional evolution Galerkin schemes have been derived by Zahaykah. The EG-methods or the finite volume EG methods were applied to the Maxwell equations, the Euler equations of gas dynamics, shallow water magnetohydrodynamic equations as well as to the shallow water equations with source terms, see [16], [18], [19], [9], [20]. Higher order finite volume evolution Galerkin (FVEG) methods have been introduced and studied in [15], [17], [18], [21], where the sharp shock-capturing properties are demonstrated as well.

[1]TU Hamburg-Harburg, Arbeitsbereich Mathematik, Schwarzenbergstrasse 95, 21 073 Hamburg, Germany, email: lukacova@tu-harburg.de

[2]Institut für Analysis und Numerik, Otto-von-Guericke-Universität Magdeburg, Universitätsplatz 2, 39 106 Magdeburg, Germany, emails: Gerald.Warnecke@mathematik.uni-magdeburg.de, Yousef.Zahaykah@mathematik.uni-magdeburg.de

[3]Department of Mathematics, Al Quds University, Jerusalem, Palestine

Theoretical error analysis of the FVEG schemes was done for the linearized systems of hyperbolic conservation laws in [18]. It has been shown that if a bilinear recovery is used the method is of the second order in time and space. New approximate evolution operators developed in [14] improved stability of the whole finite volume EG scheme, yielding the stability limit which is close to a natural limit of CFL=1; see also [22] for stability study using the Fourier analysis. In general, relatively high global accuracy of the FVEG schemes in comparison to commonly used schemes has been noticed and confirmed by an extensive numerical treatment [16], [18], [14]. In particular, we have shown that the FVEG schemes derived in [14] are approximately 6-7 times more accurate than the Lax-Wendroff scheme or the wave propagation algorithm of LeVeque [12]. In [27], [28] generalization of the FVEG schemes on unstructured triangular grids has been realized.

The main objective of this paper is to demonstrate the applicability of theory of bicharacteristics in order to construct numerical methods for three-dimensional problems. We start in this paper with a linear system of wave equation, which describes propagation of three-dimensional acoustic waves. This study is, analogously to our previous papers for two-dimensional systems of hyperbolic conservation laws, an important preparatory step in order to consider three-dimensional Euler equations of gas dynamics, which is our future goal.
In order to derive the FVEG scheme for three-dimensional wave equation system we start with the derivation of exact integral equations, which are based on the theory of bicharacteristics. Applying numerical quadratures we derive the approximate evolution operators. The latter are used in order to predict solution at cell interfaces. Afterwards, in the corrector step the finite volume update is applied.

The outline of this paper is as follows: in the next section we briefly describe the general theory used to derive the exact integral equations. In Section 3 we introduce the finite volume evolution Galerkin schemes. The exact integral equations as well as the approximate evolution operators for the three-dimensional wave equation system are given in Section 4. The derivation of the first-order schemes is given in Section 5. In Section 6 numerical tests, which demonstrate the accuracy and the multidimensionality of our schemes, are presented. Finally in Section 7 we define further new FVEG schemes based on neglecting the so-called source term, we test and discuss their accuracy.

2 General Theory

In this section we recall the derivation of the exact integral equations for a general linear hyperbolic system using the concept of bicharacteristics. The general form of the linear hyperbolic system is given as

$$\mathbf{u}_t + \sum_{k=1}^{d} \mathcal{A}_k \mathbf{u}_{x_k} = 0, \;\; \mathbf{x} = (x_1, \ldots, x_d)^T \in \mathbb{R}^d \tag{2.1}$$

where the coefficient matrices $\mathcal{A}_k, k = 1, ..., d$, are elements of $\mathbb{R}^{p\times p}$and the dependent variables are $\mathbf{u} = (u_1, ..., u_p)^T = \mathbf{u}(\mathbf{x}, t) \in \mathbb{R}^p$. Let $\mathcal{A}(\mathbf{n}) = \sum_{k=1}^{d} n_k \mathcal{A}_k$ be the pencil matrix, where $\mathbf{n} = (n_1, ..., n_d)^T$ is a directional vector in $\mathbb{R}^d$. The matrix $\mathcal{A}(\mathbf{n})$ has p real eigenvalues λ_k, $k =$

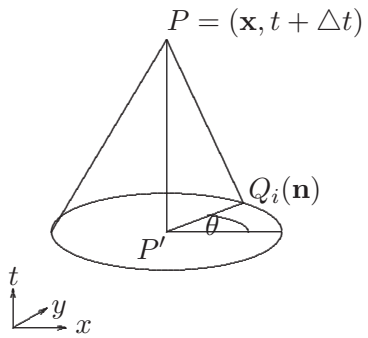

Figure 1: Bicharacteristics along the Mach cone through P and $Q_i(\mathbf{n})$, $d = 2$.

$1, ..., p$, and p corresponding linearly independent right eigenvectors $\mathbf{r}_k = \mathbf{r}_k(\mathbf{n})$, $k = 1, ..., p$. Let $\mathcal{R} = [\mathbf{r}_1|\mathbf{r}_2|...|\mathbf{r}_p]$ be the matrix of right eigenvectors then we can define the characteristic variable $\mathbf{w} = \mathbf{w}(\mathbf{n})$ as $\partial\mathbf{w}(\mathbf{n}) = \mathcal{R}^{-1}\partial\mathbf{u}$. Since system (2.1) has constant coefficient matrices $\mathcal{A}_k$ we have $\mathbf{w} = \mathcal{R}^{-1}\mathbf{u}$ or $\mathbf{u} = \mathcal{R}\,\mathbf{w}$. Multiplying equation (2.1) by $\mathcal{R}^{-1}$ from the left we get

$$\mathcal{R}^{-1}\mathbf{u}_t + \sum_{k=1}^{d} \mathcal{R}^{-1}\mathcal{A}_k\mathcal{R}\,\mathcal{R}^{-1}\mathbf{u}_{x_k} = 0. \tag{2.2}$$

Let $\mathcal{B}_k = \mathcal{R}^{-1}\mathcal{A}_k\mathcal{R} = (b_{ij}^k)_{i,j=1}^p$, where $k = 1, 2, ..., d$, then the equation (2.2) can be rewritten in the following form

$$\mathbf{w}_t + \sum_{k=1}^{d} \mathcal{B}_k\mathbf{w}_{x_k} = 0.$$

Let us introduce the decomposition $\mathcal{B}_k{=}\mathcal{D}_k{+}\mathcal{B}'_k$, where $\mathcal{D}_k$ contains the diagonal part of the matrix $\mathcal{B}_k$. This yields

$$\mathbf{w}_t + \sum_{k=1}^{d} \mathcal{D}_k\mathbf{w}_{x_k} = -\sum_{k=1}^{d} \mathcal{B}'_k\mathbf{w}_{x_k} =: \mathbf{s}. \tag{2.3}$$

The i-th bicharacteristic corresponding to the i-th equation of (2.3) is defined by

$$\frac{d\mathbf{x}_i}{d\tilde{t}} = \mathbf{b}_{ii}(\mathbf{n}) = (b_{ii}^1, b_{ii}^2, ..., b_{ii}^d)^T,$$

where $i = 1, ..., p$. Here b_{ii}^k are the diagonal entries of the matrix $\mathcal{B}_k$, $k = 1, ..., d$, $i = 1, ..., p$. We consider the bicharacteristics backwards in time. Therefore the initial conditions are $\mathbf{x}_i(t + \Delta t, \mathbf{n}) = \mathbf{x}$ for all $\mathbf{n} \in \mathbb{R}^d$ and $i = 1, ..., p$, i.e. $\mathbf{x}_i(\tilde{t}, \mathbf{n}) = \mathbf{x} - \mathbf{b}_{ii}(\mathbf{n})(t + \Delta t - \tilde{t})$.
We will integrate the i-th equation of the system (2.3) from the point P down to the point $Q_i(\mathbf{n}) := Q_i(\mathbf{x}_i(\mathbf{n}, t), t)$, where the bicharacteristic hits the basic plane, see Figure 1. Note that bicharacteristics are straight lines because the system is linear with constant coefficients. Now the i-th equation reads

$$\frac{\partial w_i}{\partial t} + \sum_{k=1}^{d} b_{ii}^k \frac{\partial w_i}{\partial x_k} = -\left(\sum_{j=1, i\neq j}^{d} \left(b_{ij}^1 \frac{\partial w_j}{\partial x_1} + b_{ij}^2 \frac{\partial w_j}{\partial x_2} + ... + b_{ij}^d \frac{\partial w_j}{\partial x_d}\right)\right) = s_i, \tag{2.4}$$

where $P \equiv (\mathbf{x}, t+\Delta t) \in \mathbb{R}^p \times \mathbb{R}_+$ is taken to be a fixed point, while $Q_i(\mathbf{n}) = (\mathbf{x} - \Delta t \mathbf{b}_{ii}, t)$. Taking a vector $\sigma_i = (b_{ii}^1, b_{ii}^2, ..., b_{ii}^d, 1)$, we can define the directional derivative

$$\frac{dw_i}{d\sigma_i} = \left(\frac{\partial w_i}{\partial x_1}, \frac{\partial w_i}{\partial x_2}, ..., \frac{\partial w_i}{\partial x_d}, \frac{\partial w_i}{\partial t} \right) \cdot \sigma_i = \frac{\partial w_i}{\partial t} + b_{ii}^1 \frac{\partial w_i}{\partial x_1} + b_{ii}^2 \frac{\partial w_i}{\partial x_2} + ... + b_{ii}^d \frac{\partial w_i}{\partial x_d}.$$

Hence the i-th equation (2.4) can be rewritten as follows:

$$\frac{dw_i}{d\sigma_i} = s_i = - \sum_{j=1, i \neq j}^{d} \left(b_{ij}^1 \frac{\partial w_j}{\partial x_1} + b_{ij}^2 \frac{\partial w_j}{\partial x_2} + ... + b_{ij}^d \frac{\partial w_j}{\partial x_d} \right).$$

Now the integration from P to $Q_i(\mathbf{n})$ gives

$$w_i(P) - w_i(Q_i(\mathbf{n}), \mathbf{n}) = s_i', \tag{2.5}$$

where

$$s_i' = \int_t^{t+\Delta t} s_i(\mathbf{x}_i(\tilde{t}, \mathbf{n}), \tilde{t}) d\tilde{t} = \int_0^{\Delta t} s_i(\mathbf{x}_i(\tau, \mathbf{n}), t + \Delta t - \tau) \mathrm{d}\tau.$$

Multiplication of equation (2.5) by $\mathcal{R}$ from the left and $(d-1)-$dimensional integration of the variable $\mathbf{n}$ over the unit sphere O in $\mathbb{R}^d$ leads to the exact integral equations for (2.1)

$$\mathbf{u}(P) = \mathbf{u}(\mathbf{x}, t+\Delta t) = \frac{1}{|O|} \int_O \mathcal{R}(\mathbf{n}) \begin{pmatrix} w_1(Q_1(\mathbf{n}), \mathbf{n}) \\ w_2(Q_2(\mathbf{n}), \mathbf{n}) \\ w_3(Q_3(\mathbf{n}), \mathbf{n}) \\ \vdots \\ w_p(Q_p(\mathbf{n}), \mathbf{n}) \end{pmatrix} \mathrm{d}O + \tilde{\mathbf{s}}, \tag{2.6}$$

where

$$\tilde{\mathbf{s}} = (\tilde{s}_1, \tilde{s}_2, ..., \tilde{s}_p)^T = \frac{1}{|O|} \int_O \mathcal{R}(\mathbf{n}) \mathbf{s}' \mathrm{d}O = \frac{1}{|O|} \int_O \int_0^{\Delta t} \mathcal{R}(\mathbf{n}) \mathbf{s}(\mathbf{x}_i(\tau, \mathbf{n}), t + \Delta t - \tau) \mathrm{d}\tau \mathrm{d}O$$

and $|O|$ corresponds to the measure of the domain of integration.

3 Evolution Galerkin Schemes

In this section we recall the definition of the finite volume evolution Galerkin (FVEG) schemes. We assume that $d = 3$ and Δx, Δy, $\Delta z > 0$ are the mesh size parameters in the $x-, y-, z-$ direction, respectively. We construct a regular mesh, which consists of the mesh cells

$$\begin{aligned} \Omega_{klm} &= \left[(k - \frac{1}{2})\Delta x, (k + \frac{1}{2})\Delta x \right] \times \left[(l - \frac{1}{2})\Delta y, (l + \frac{1}{2})\Delta y \right] \times \left[(m - \frac{1}{2})\Delta z, (m + \frac{1}{2})\Delta z \right] \\ &= \left[x_k - \frac{\Delta x}{2}, x_k + \frac{\Delta x}{2} \right] \times \left[y_l - \frac{\Delta y}{2}, y_l + \frac{\Delta y}{2} \right] \times \left[z_m - \frac{\Delta z}{2}, z_m + \frac{\Delta z}{2} \right], \end{aligned}$$

where $k, l, m \in \mathbb{Z}$. Suppose that S_h^q is a finite element space consisting of piecewise polynomials of degree $q \geq 0$ with respect to the mesh and assume constant time step, i.e. $t_n = n\Delta t$. Let $\mathbf{U}^n$ be an approximation in the space S_h^q to the exact solution $\mathbf{u}(., t_n)$ at time $t_n \geq 0$. We denote by $R_h : S_h^q \to S_h^r$ a recovery operator, $r > q \geq 0$ and by E_τ the so-called approximate evolution operator, which is a suitable approximation to the exact evolution operator defined by the integral equation (2.6). In the next section such approximate evolution operators are derived for the wave equation system.

Definition 3.1 *Starting from some initial data* $\mathbf{U}^0 \in S_h^q$*, the finite volume evolution Galerkin method (FVEG) is recursively defined by means of*

$$\mathbf{U}^{n+1} = \mathbf{U}^n - \int_0^{\Delta t} \sum_{j=1}^{3} \frac{1}{\Delta_{x_j}} \delta_{x_j} \mathbf{f}_j(\tilde{\mathbf{U}}^{n+\frac{\tau}{\Delta t}}) d\tau, \tag{3.2}$$

where we use the equivalent notation for the space variables $(x, y, z) = (x_1, x_2, x_3)$ *and denote by* $\delta_{x_j} \mathbf{f}_j(\tilde{\mathbf{U}}^{n+\frac{\tau}{\Delta t}})$ *an approximation to the face flux difference;* δ_x *is defined by* $\delta_x = v(x + \frac{\Delta x}{2}) - v(x - \frac{\Delta x}{2})$*. The cell boundary value* $\tilde{\mathbf{U}}^{n+\frac{\tau}{\Delta t}}$ *is evolved using the approximate evolution operator* E_τ *to* $t_n + \tau$ *and averaged along the cell boundary, i.e.*

$$\tilde{\mathbf{U}}^{n+\frac{\tau}{\Delta t}} = \sum_{k,l,m \in \mathbb{Z}} \left(\frac{1}{|\partial\Omega_{klm}|} \int_{\partial\Omega_{klm}} E_\tau R_h \mathbf{U}^n dS \right) \chi_{\partial\Omega_{klm}}, \tag{3.3}$$

where $\chi_{\partial\Omega_{klm}}$ *is the characteristic function of* $\partial\Omega_{klm}$*.*

It is important to note that in the update step (3.2) numerical quadrature rules are used instead of the exact time integration. In this paper we are using the midpoint rule for the time integration in (3.2). Similarly, to evaluate the intermediate value $\tilde{\mathbf{U}}^{n+\frac{\tau}{\Delta t}}$ in (3.3) the three-dimensional integrals along the cell face are evaluated by means of suitable numerical quadrature rules, e.g. the trapezoidal rule is used in the numerical experiments below. The integrals aroud the unit sphere O, which arrive from E_τ, are evaluated exactly. In this way all of the infinitely many directions of wave propagation are taken into account explicitly.

4 Exact Integral Equations and Approximate Evolution Operators for the Wave Equation System

In this section we derive two first-order approximate evolution operators for the three-dimensional wave equation system. We begin by applying the general theory given in Section 2. It is well known that the wave equation can be written as a first-order system of partial differential equations in the form

$$\begin{aligned} \phi_t + c\nabla \cdot \mathbf{v} &= 0, \\ \mathbf{v}_t + c\nabla\phi &= 0, \end{aligned} \tag{4.1}$$

where c is a constant, the speed of sound, and $\mathbf{v}(\mathbf{x}, t) := (u, v, w)^T(\mathbf{x}, t)$, $(\mathbf{x}, t) \in \mathbb{R}^3 \times \mathbb{R}^+$ is the velocity field. Let $\mathbf{u} := (\phi, \mathbf{v})^T$ be the vector of the unknown variables and let the fluxes be $\mathbf{f}_1(\mathbf{u}) := (c\,u, c\,\phi, 0, 0)^T$, $\mathbf{f}_2(\mathbf{u}) := (c\,v, 0, c\,\phi, 0)^T$ and $\mathbf{f}_3(\mathbf{u}) := (c\,w, 0, 0, c\,\phi)^T$. The system (4.1) can be written in the conservation form

$$\frac{\partial \mathbf{u}}{\partial t} + \sum_{k=1}^{3} \frac{\partial \mathbf{f}_k(\mathbf{u})}{\partial x_k} = 0. \tag{4.2}$$

Using Jacobian matrices of the flux functions we can rewrite system (4.2) in the linearized form

$$\mathbf{u}_t + \mathcal{A}_1 \mathbf{u}_x + \mathcal{A}_2 \mathbf{u}_y + \mathcal{A}_3 \mathbf{u}_z = 0. \tag{4.3}$$

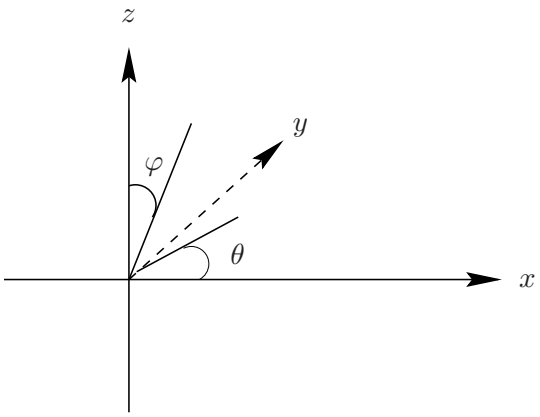

Figure 2: Spherical coordinates.

Let $\mathbf{n} := (n_1, n_2, n_3)^T := (\cos\theta\sin\varphi, \sin\theta\sin\varphi, \cos\varphi)^T$ be a directional vector in $\mathbb{R}^3$ with $\theta \in [0, 2\pi]$ and $\varphi \in [0, \pi]$, see Fig 2. Then the system (4.3) has four real eigenvalues $\lambda_1 = -c, \lambda_2 = 0, \lambda_3 = 0, \lambda_4 = c$ and four corresponding right eigenvectors

$$\mathbf{r}_1 = \begin{pmatrix} -1 \\ \mathbf{n} \end{pmatrix}, \mathbf{r}_2 = \begin{pmatrix} 0 \\ n_2 \\ -n_1 \\ 0 \end{pmatrix}, \mathbf{r}_3 = \begin{pmatrix} 0 \\ n_3 \\ 0 \\ -n_1 \end{pmatrix}, \mathbf{r}_4 = \begin{pmatrix} 1 \\ \mathbf{n} \end{pmatrix}.$$

The vector of characteristic variables $\mathbf{w} = (w_1, w_2, w_3, w_4)^T$ is given as

$$\mathbf{w}(\mathbf{n}) = \mathcal{R}^{-1}(\mathbf{n})\mathbf{u} = \begin{bmatrix} \frac{1}{2}\mathbf{u}\cdot\mathbf{r}_1 \\ \frac{1}{n_1^2}\mathbf{u}\cdot[(n_1^2+n_3^2)\mathbf{r}_2 - n_2n_3\mathbf{r}_3] \\ \frac{1}{n_1^2}\mathbf{u}\cdot[-n_2n_3\mathbf{r}_2 + (n_1^2+n_2^2)\mathbf{r}_3] \\ \frac{1}{2}\mathbf{u}\cdot\mathbf{r}_4 \end{bmatrix}. \tag{4.4}$$

To determine the points $Q_i(\mathbf{n})$, $i = 1, 2, 3, 4$, recall that the bicharacteristics $\mathbf{x}_i$, which correspond to this system are given as $\frac{d\mathbf{x}_i}{d\tilde{t}} = \mathbf{b}_{ii} = (b_{ii}^1, b_{ii}^2, b_{ii}^3)^T, i = 1, 2, 3, 4$. Hence we get $\mathbf{x}_i(\mathbf{n}, \tilde{t}) = \mathbf{x} - \mathbf{b}_{ii}(t + \Delta t - \tilde{t})$. Therefore we have for the footpoints of the bicharacteristics $Q_i(\mathbf{x}_i(\mathbf{n}, t), t) = (\mathbf{x} - \mathbf{b}_{ii}\Delta t, t)$. From the diagonal matrices $\mathcal{D}_1$, $\mathcal{D}_2$, $\mathcal{D}_3$, see Section 2, we get $\mathbf{b}_{11} = -c\mathbf{n}$, $\mathbf{b}_{22} = \mathbf{b}_{33} = \mathbf{0}$ and $\mathbf{b}_{44} = c\mathbf{n}$. Hence

$$\begin{aligned} Q_2 \equiv Q_3 \quad &\text{correspond to} \quad \lambda_{2,3} = 0, \\ Q_1 \quad &\text{corresponds to} \quad \lambda_1 = -c, \\ Q_4 \quad &\text{corresponds to} \quad \lambda_4 = c. \end{aligned}$$

Using symmetry between the points Q_1 and Q_4 and the property that the characteristic variables are periodic we can derive the integral equations that are equivalent to the wave equation system in three dimensions (4.1). In the next lemma we give these integral equations. Let $\mathcal{J} = [\mathbf{J}_0|\mathbf{J}_1|\mathbf{J}_2|\mathbf{J}_3]$ be the matrix whose columns are the vectors $\mathbf{J}_0 = (0,0,0)^T$, $\mathbf{J}_1 = (-1,0,0)^T + n_1\mathbf{n}$, $\mathbf{J}_2 = (0,-1,0)^T + n_2\mathbf{n}$, $\mathbf{J}_3 = (0,0,-1)^T + n_3\mathbf{n}$. Set $\tilde{P} = (\mathbf{x}, t + \Delta t - \tau)$, $\tilde{Q} = (\mathbf{x} + c\tau\mathbf{n}, t + \Delta t - \tau)$, $P = (\mathbf{x}, t + \Delta t)$, $Q = (\mathbf{x} + c\Delta t\mathbf{n}, t)$ and $P' = (\mathbf{x}, t)$, where $\tau \in [0, \Delta t]$. Then using some invariance properties for terms in spherical coordinates we get

Lemma 4.5 *The exact integral representation (3.2) for the wave equation system (4.1) reads*

$$\mathbf{u}(P) = \left(\frac{d-1}{d}\right)\mathbf{u}'(P') + \frac{1}{|O|}\int_O \mathbf{u}(Q)\cdot(-1,\mathbf{n})^T(-1,\mathbf{n})^T\,dS + \tilde{\mathbf{s}}, \tag{4.6}$$

where d is the dimension, i.e. $d=3$ in our case, $\mathbf{u}'(P') = (0,\mathbf{v})^T(P')$ and

$$\tilde{\mathbf{s}} = \frac{1}{|O|}\int_O\int_0^{\Delta t}\left((-1,\mathbf{n})^T\,s(\tilde{Q}) + c\nabla\phi(\tilde{P})\mathcal{J}\right)\mathrm{d}\tau\mathrm{d}S, \tag{4.7}$$

$$s = \frac{c}{1-n_3^2}\left(n_2^2u_x - n_1n_2(u_y+v_x) + n_1^2v_y\right) + \frac{1}{\tau}\frac{d\mathbf{n}}{d\varphi}\cdot\frac{d\mathbf{v}}{d\varphi}, \tag{4.8}$$

$$c\nabla\phi(\tilde{P})\mathcal{J} = (c\nabla\phi\cdot\mathbf{J}_0,\, c\nabla\phi\cdot\mathbf{J}_1,\, c\nabla\phi\cdot\mathbf{J}_2,\, c\nabla\phi\cdot\mathbf{J}_3)^T.$$

Proof: See[29]. □

Remark 4.9 *Since the point $\tilde{P}$ is independent of the directional vector $\mathbf{n}$ we can evaluate the second part of the integral (4.7) to get $\left(\frac{1-d}{d}\right)(\mathbf{u}'(P') - \mathbf{u}'(P))$. Then substituting in the equation (4.6) and rearranging the terms we get the equivalent system of the exact integral equations*

$$\mathbf{u}(P) = \frac{k}{|O|}\int_O \mathbf{u}(Q)\cdot(-1,\mathbf{n})^T(-1,\mathbf{n})^T\,dS + k\tilde{\mathbf{s}}, \tag{4.10}$$

where $\tilde{\mathbf{s}}$ is given as

$$\tilde{\mathbf{s}} = \frac{1}{|O|}\int_O\int_0^{\Delta t}(-1,\mathbf{n})^T\,s(\tilde{Q})\,d\tau\,dS, \tag{4.11}$$

s is given in the equation (4.8). For the first component of the vector $\mathbf{u}$, i.e. for ϕ, we have $k=1$, otherwise $k=d$.

To obtain explicit numerical methods we approximate time integrals in equations (4.7) and (4.11) using the backward rectangle rule, which gives

$$\tilde{\mathbf{s}} = \frac{\Delta t}{|O|}\int_O\left((-1,\mathbf{n})^T\,s(Q) + c\nabla\phi(P')\mathcal{J}\right)\mathrm{d}\tau\mathrm{d}S + \mathcal{O}(\Delta t^2), \tag{4.12}$$

$$\tilde{\mathbf{s}} = \frac{\Delta t}{|O|}\int_O(-1,\mathbf{n})^T\,s(Q)\,\mathrm{d}\tau\mathrm{d}S + \mathcal{O}(\Delta t^2), \tag{4.13}$$

respectively. In order to evaluate the integral of the source terms s we need the following lemma. The proof can be found in [29].

Lemma 4.18

$$\Delta t \int_O s(Q)\,dS = \int_O (2n_1u(Q) + 2n_2v(Q) + 2n_3w(Q))\,dS, \tag{4.19}$$

$$\Delta t \int_O n_1 s(Q)\,dS = \int_O \left((-1+3n_1^2)u(Q) + 3n_1n_2v(Q) + 3n_1n_3w(Q)\right)\,dS, \tag{4.20}$$

$$\Delta t \int_O n_2 s(Q)\,dS = \int_O \left(3n_1n_2u(Q) + (-1+3n_2^2)v(Q) + 3n_2n_3w(Q)\right)\,dS, \tag{4.21}$$

$$\Delta t \int_O n_3 s(Q)\,dS = \int_O \left(3n_1n_3u(Q) + 3n_2n_3v(Q) + (-1+3n_3^2)w(Q)\right)\,dS. \tag{4.22}$$

□

Using Taylor's theorem we can approximate the integral of the second term in the equation (4.12), which yields

$$\int_O c\nabla\phi(P')\cdot\mathbf{J}_1 \mathrm{d}S = \int_O -2n_1\phi(Q)\mathrm{d}S + \mathcal{O}(\Delta t^2), \tag{4.23}$$

$$\int_O c\nabla\phi(P')\cdot\mathbf{J}_2 \mathrm{d}S = \int_O -2n_2\phi(Q)\mathrm{d}S + \mathcal{O}(\Delta t^2), \tag{4.24}$$

$$\int_O c\nabla\phi(P')\cdot\mathbf{J}_3 \mathrm{d}S = \int_O -2n_3\phi(Q)\mathrm{d}S + \mathcal{O}(\Delta t^2). \tag{4.25}$$

Let $\mathcal{I}(m) = [\mathbf{I}_0|\mathbf{I}_1|\mathbf{I}_2|\mathbf{I}_3]$, $m \in \{1,3\}$, be the matrix with the column vectors

$$\begin{aligned}
\mathbf{I}_0 &= (0,0,0,0)^T + (1,-3\mathbf{n})^T,\\
\mathbf{I}_1 &= (0,-1,0,0)^T + n_1(-m,4\mathbf{n})^T,\\
\mathbf{I}_2 &= (0,0,-1,0)^T + n_2(-m,4\mathbf{n})^T,\\
\mathbf{I}_3 &= (0,0,0,-1)^T + n_3(-m,4\mathbf{n})^T.
\end{aligned}$$

Substituting equations (4.19-4.25) in the equation (4.6) we get the following approximate evolution operator, which we call the **EG3 for 3D**, cf. [16]

$$\mathbf{u}(P) = \left(\frac{d-1}{d}\right)\mathbf{u}'(P') + \frac{1}{|O|}\int_O \mathbf{u}(Q)\mathcal{I}(3)\mathrm{d}S + \mathcal{O}(\Delta t^2), \tag{4.26}$$

where $\mathbf{U}(Q)\mathcal{I}(3) = \phi(Q)\mathbf{I}_0 + u(Q)\mathbf{I}_1 + v(Q)\mathbf{I}_2 + w(Q)\mathbf{I}_3$.

Remark 4.27 *Substituting equations (4.19-4.22) in the equation (4.10) we get the following approximate evolution operator*

$$\mathbf{u}(P) = \frac{k}{|O|}\int_O \mathbf{u}(Q)\mathcal{I}(1)\,dS + \mathcal{O}(\Delta t^2), \tag{4.28}$$

where $\mathbf{U}(Q)\mathcal{I}(1)$ *is defined analogously as* $\mathbf{U}(Q)\mathcal{I}(3)$*. This approximate evolution operator is analogous to the two-dimensional approximate operator EG1, cf. [16].*

5 Numerical Schemes and Discretization

This section is devoted to the numerical experiments using the finite volume EG scheme based on the approximate evolution operator (4.26) and on Definition 3.1. Analogously to the two-dimensional case, cf. [29], we use the midpoint rule to approximate the time integral in the equation (3.2) and the trapezoidal rule to approximate the cell face integrals given in (3.3). Let $\tilde{\mathbf{U}}_l$ denote the intermediate value corresponding to the left side of the cell ijk, see Figure 3. Further, let $\tilde{\mathbf{U}}_f$ and $\tilde{\mathbf{U}}_b$ be the intermediate values corresponding to the front and to the bottom sides, respectively. Let N_x, N_y and N_z be the number of cells along the $x-$, $y-$ and $z-$axis, respectively; recall that Δx, Δy, Δz are the mesh steps in the corresponding directions. Then the first-order evolution Galerkin algorithm is formulated as follows:

- *input of the initial data* $\mathbf{U}^0$.
- *determine the time step* Δt *from the CFL condition* $\frac{c\Delta t}{\min\{\Delta x,\Delta y,\Delta z\}} = \nu < 1$.
- *do the time loop*
  - *calculate the intermediate values* $\tilde{\phi}_l$, $\tilde{u}_l$, $\tilde{\phi}_f$, $\tilde{v}_f$, $\tilde{\phi}_b$, $\tilde{w}_b$ *according (3.3) using the approximate evolution operator EG3-3D, cf. (4.26)*
  - *FV update:*

$$\begin{aligned}
\phi_{ijk}^{n+1} &= \phi_i^n - \frac{c\Delta t}{\Delta x}\left(\tilde{u}_l(i+1jk) - \tilde{u}_l(ijk)\right) - \frac{c\Delta t}{\Delta y}\left(\tilde{v}_f(ij+1k) - \tilde{v}_f(ijk)\right) \\
&\quad - \frac{c\Delta t}{\Delta z}\left(\tilde{w}_b(ijk+1) - \tilde{w}_b(ijk)\right), \qquad (5.1)\\
u_{ijk}^{n+1} &= u_i^n - \frac{c\Delta t}{\Delta x}\left(\tilde{\phi}_l(i+1jk) - \tilde{\phi}_l(ijk)\right), \qquad (5.2)\\
v_{ijk}^{n+1} &= v_i^n - \frac{c\Delta t}{\Delta y}\left(\tilde{\phi}_f(ij+1k) - \tilde{\phi}_f(ijk)\right), \qquad (5.3)\\
w_{ijk}^{n+1} &= w_i^n - \frac{c\Delta t}{\Delta z}\left(\tilde{\phi}_b(ijk+1) - \tilde{\phi}_b(ijk)\right). \qquad (5.4)
\end{aligned}$$

- *impose the boundary conditions.*
- *end of the time loop.*

This is the so-called FVEG3-3D scheme; note that the analogous numerical schemes based on the approximate evolution operator (4.28) can be derived. Finally, we note that in the experiments presented below we evaluate the intermediate values $\tilde{\mathbf{U}}$ on cell faces by using the piecewise constant approximate functions, i.e. the scheme is first-order in space. Apparently, the presented discrete EG schemes are explicit in time, which implies that some stability condition needs to be satisfied in order to guarantee stability of the schemes. It should be noted that we have studied the question of stability of the EG as well as the FVEG schemes extensively in [14, 22]. It has been shown there that the EG schemes are stable under some stability conditions with the CFL number close to a natural limit of 1.0, see [14, 22] for more details.

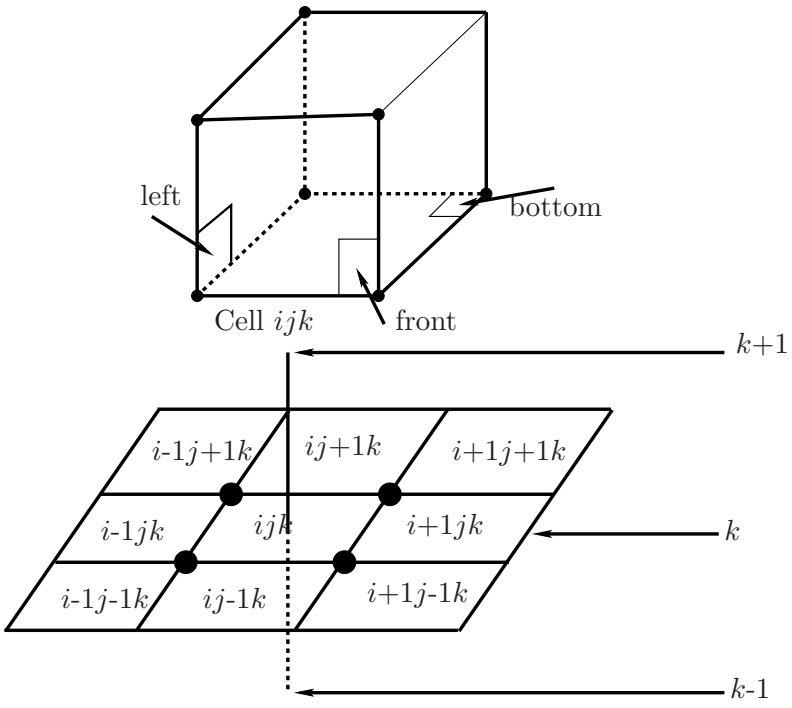

Figure 3: Cell ijk and its neighbours

Remark 5.5

The derivation of FVEG schemes might be consider at a first sight as a rather complex task. However, the implementation is divided into several simpler subtasks as indicated above. The flux integrals along cell interfaces are approximated by the trapezoidal rule. At each integration point at cell interfaces the corresponding approximate evolution operator (4.26), (4.28), (7.1) and (7.2) is implemented directly. The only complexity lies in the implementation of the exact integrals with integrands being a combination of $\sin\theta\sin\varphi$, $\cos\theta\sin\varphi$ and $\cos\varphi$ over $[\theta_1,\theta_2]\times[\varphi_1,\varphi_2]$ according to the position of the Mach cone. In order to simplify the implementation task, e.g. in the case of full three-dimenionsional Euler equations, the integrals over the sonic ball, i.e. over $[0,2\pi]\times[0,\pi]$, can be approximated alternatively by suitable numerical quadratures.

6 Numerical Tests

Example 6.1

Consider the three dimensional wave equation system together with the periodic boundary conditions and the initial data

$$\begin{aligned}\phi(x,y,0) &= -\frac{1}{c}(\sin(2\pi x)+\sin(2\pi y)+\sin(2\pi z)),\\ u(x,y,0) &= v(x,y,0)=w(x,y,0)=0.\end{aligned} \tag{6.2}$$

where $(x, y, z) \in [-1, 1] \times [-1, 1] \times [-1, 1]$. The exact solution is

$$\begin{aligned} \phi(x, y, t) &= -\frac{1}{c}\cos(2\pi ct)(\sin(2\pi x) + \sin(2\pi y) + \sin(2\pi z)), \\ u(x, y, t) &= \frac{1}{c}\sin(2\pi ct)\cos(2\pi x), \\ v(x, y, t) &= \frac{1}{c}\sin(2\pi ct)\cos(2\pi y), \\ w(x, y, t) &= \frac{1}{c}\sin(2\pi ct)\cos(2\pi z). \end{aligned} \tag{6.3}$$

The following two tables show the L^2-error and the experimental order of convergence (EOC), which is defined using two solutions computed on meshes of sizes N_1, N_2, as follows

$$\text{EOC} = \ln \frac{\|\mathbf{U}_{N_1}(T) - \mathbf{U}^n_{N_1}\|}{\|\mathbf{U}_{N_2}(T) - \mathbf{U}^n_{N_2}\|} / \ln\left(\frac{N_2}{N_1}\right).$$

The numerical experiments are carried out with the FVEG3-3D scheme. We take the final time $T = 0.1$ and $T = 0.2$, respectively, and set the constant c equal to 1. Moreover we consider a uniform mesh, i.e. we take the mesh size $h > 0$, $h = \Delta x = \Delta y = \Delta z$, and set the CFL number to be 0.5. The last column of Tables 1 and 2 demonstrates that the experimental order of convergence is 1.

N	$\|\phi(T) - \phi^n\|$	$\|u(T) - u^n\|$	$\|\mathbf{U}(T) - \mathbf{U}^n\|$	EOC
20	0.55892402464	0.16838548872	0.63044197493	
40	0.27817890698	0.09911167224	0.32688358021	0.9476
80	0.13874739504	0.05362621166	0.16696751589	0.9692
160	0.06927101055	0.02788768195	0.08444904569	0.9834
320	0.03460647659	0.01422055263	0.04247682396	0.9914

Table 1: FVEG3-3D scheme, T=0.1, CFL=0.5

N	$\|\phi(T) - \phi^n\|$	$\|u(T) - u^n\|$	$\|\mathbf{U}(T) - \mathbf{U}^n\|$	EOC
20	0.49587434262	0.59746694762	1.14751541347	
40	0.23446528786	0.33325251909	0.62301339926	0.8812
80	0.11224035516	0.17664332961	0.32589337983	0.9349
160	0.05458773142	0.09102322692	0.16683975527	09659
320	0.02686871668	0.04621317753	0.08443282103	0.9826

Table 2: FVEG3-3D scheme, T=0.2, CFL=0.5

In Figures 4 we plot the first and the second components of the solution $\phi(x, 0.5, 0.5, T)$ and $u(x, 0.5, 0.5, T)$ (on top and on bottom, respectively) restricted to a horizontal line for a $80 \times 80 \times 80$ and a $320 \times 320 \times 320$ mesh at the end time $T = 0.2$. The exact solution is plotted as well. We can notice a good agreement between the approximate and the exact solution.

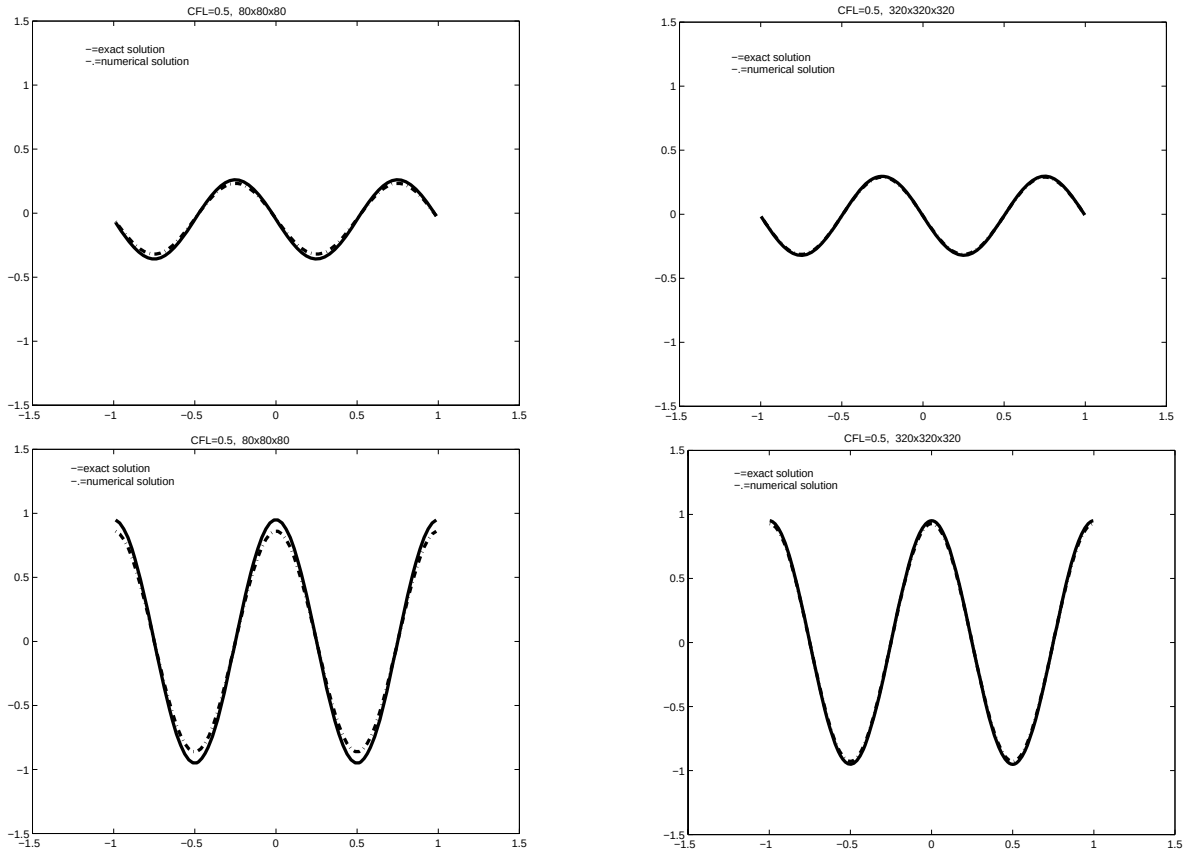

Figure 4: Solution of the wave equation system computed using the $80 \times 80 \times 80$ mesh cells (left) and $320 \times 320 \times 320$ mesh cells (right); top: $\phi(x, 0.5, 0.5, 0.2)$, bottom: $u(x, 0.5, 0.5, 0.2)$.

Example 6.4

It is easy to see that the wave equation system preserves exactly the vorticity, i.e. the vector $\left(\frac{\partial u}{\partial y} - \frac{\partial v}{\partial x}, \frac{\partial u}{\partial z} - \frac{\partial w}{\partial x}, \frac{\partial v}{\partial z} - \frac{\partial w}{\partial y}\right)^T$ is constant in time. Components of vorticity vector are trivially zero in Example 6.1, because u depends on x only, v depends on y only while w depends on z only. In this example we take the following nontrivial initial data for which the exact solution still has vanishing vorticity

$$\begin{aligned} \phi(x,y,0) &= -\exp(-10(x^2+y^2+z^2)), \\ u(x,y,0) &= v(x,y,0) = w(x,y,0) = 0. \end{aligned} \tag{6.5}$$

We compute the vector of discrete vorticity given by the formulae:

$$\begin{aligned} \mathrm{DV}^{(1)}_{klm} &= \mu_x\delta_y u_{k+\frac{1}{2},l+\frac{1}{2},m-\frac{1}{2}} - \mu_y\delta_x v_{k+\frac{1}{2},l+\frac{1}{2},m-\frac{1}{2}}, \\ \mathrm{DV}^{(2)}_{klm} &= \mu_x\delta_z u_{k+\frac{1}{2},l-\frac{1}{2},m+\frac{1}{2}} - \mu_z\delta_x w_{k+\frac{1}{2},l-\frac{1}{2},m+\frac{1}{2}}, \\ \mathrm{DV}^{(3)}_{klm} &= \mu_y\delta_z v_{k-\frac{1}{2},l+\frac{1}{2},m+\frac{1}{2}} - \mu_z\delta_y w_{k-\frac{1}{2},l+\frac{1}{2},m+\frac{1}{2}} \end{aligned} \tag{6.6}$$

for each $k,l,m \in \mathbb{Z}$, where we denote by $u_{k+\frac{1}{2},l+\frac{1}{2},m-\frac{1}{2}} := u((k-\frac{1}{2})h,(l+\frac{1}{2})h,(m+\frac{1}{2})h)$ the values at the corner point $((k-\frac{1}{2})h,(l+\frac{1}{2})h,(m+\frac{1}{2})h)$ of the cubic mesh cell Ω_{kml}. The other corner-values are defined analogously. The $\mu,\delta-$operators are defined, e.g. in the $x-$direction, as

$$\delta_x f(x) = f(x+\frac{h}{2}) - f(x-\frac{h}{2}), \quad \mu_x f(x) = \frac{f(x+\frac{h}{2}) + f(x-\frac{h}{2})}{2};$$

the operators in the other directions are defined analogously. In Table 3 we show the average value of $\mathrm{DV}^{(1)}$ (average values of $\mathrm{DV}^{(2)}$ and $\mathrm{DV}^{(3)}$ are same due to the symmetry of the problem) at time $T = 0.2$ using $N = 50$, $N = 100$ and $N = 200$ mesh cells in each direction. The computational domain is a cube $[-1,1]^3$ and CFL $= 0.55$. The results in this table indicate that the FVEG3-3D preserves the discrete vorticity given by the equation (6.6). Further in the Figures 5 and 6 we plot the surface of the solution ϕ for the cross-section $z = 0.5$ and the isosurface of ϕ, respectively.

Mesh size	$50\times50\times50$	$100\times100\times100$	$200\times200\times200$
Average vorticity	1.871×10^{-5}	6.480×10^{-6}	3.350×10^{-6}

Table 3: Vorticity preservation for the FVEG3-3D scheme

7 Further EG schemes

It is well known that the solution of the wave equation in a space of odd dimension (>2) depends on the initial data distributed on the surface of the sphere centered at the observation point (Kirchhoff's formula), see [6]. We follow this concept and ignore the $\tilde{\mathbf{s}}$ part appearing

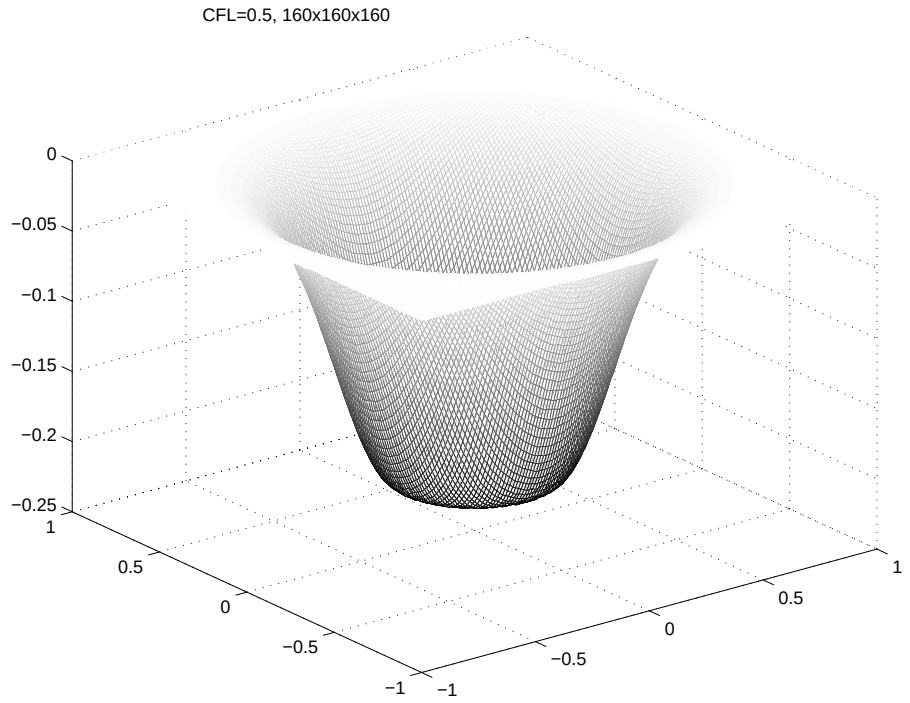

Figure 5: Cross section surfaces ($z = 0.5$) of the approximated solution ϕ at $T = 0.2$ using 160×160 mesh cells.

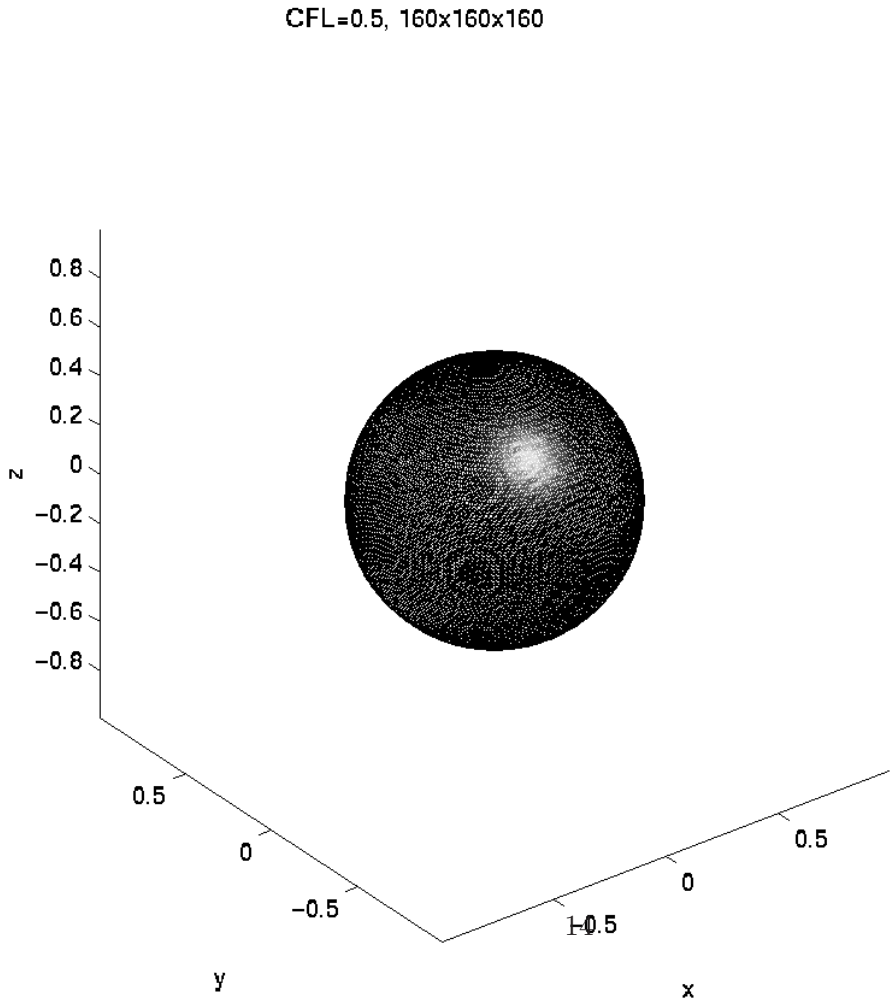

Figure 6: Isosurface of the approximated solution $\phi(x, y, z, 0.2)$ using 160×160 mesh cells.

in the exact integral equations (4.6) and (4.10). This leads us to the following approximate evolution operators:

$$\mathbf{u}(P) = \left(\frac{d-1}{d}\right)\mathbf{u}'(P') + \frac{1}{|O|}\int_O \mathbf{u}(Q)\cdot(-1,\mathbf{n})^T(-1,\mathbf{n})^T\,\mathrm{d}S, \tag{7.1}$$

$$\mathbf{u}(P) = \frac{k}{|O|}\int_O \mathbf{u}(Q)\cdot(-1,\mathbf{n})^T(-1,\mathbf{n})^T\,\mathrm{d}S. \tag{7.2}$$

We call these approximate evolution operators N1 and N2, respectively. Now, we apply the FVEG schemes based on the N1 and N2 operators to the problem given in the Example 6.1. The L^2 errors and EOC are given in Tables 4-6 and indicate superconvergence of the finite volume scheme N1. Actually using piecewise constants we have obtained an overall second order accuracy. Further, Table 6 indicates that the finite volume scheme N2 is of first order. In Figure 7 we plot the first and the second components $\phi(x, 0.5, 0.5, 0.2)$ and $u(x, 0.5, 0.5, 0.2)$ of the solution, respectively restricted to a horizontal line for $80 \times 80 \times 80$ mesh applying the second order scheme FVEG-N1. We plot also the exact solution. Comparing these plots with these given in the first column of Figure 4 we see that the FVEG-N1 scheme suffered very less dissipation as one expect.

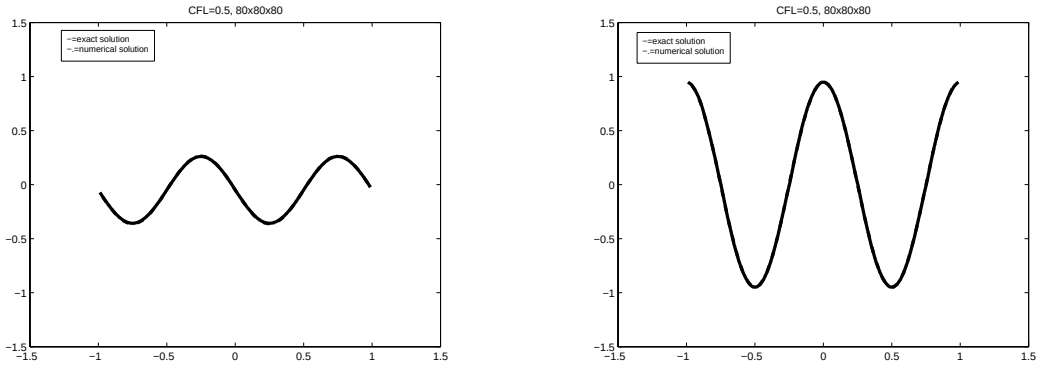

Figure 7: Solution of the wave equation system computed with FVEG-N1 scheme using $80 \times 80 \times 80$ mesh cells; left: $\phi(x, 0.5, 0.5, 0.2)$, right: $u(x, 0.5, 0.5, 0.2)$.

N	$\|\phi(T) - \phi^n\|$	$\|u(T) - u^n\|$	$\|\mathbf{U}(T) - \mathbf{U}^n\|$	EOC
20	0.03948481218	0.05612849451	0.10492985314	
40	0.01297997347	0.01347014919	0.02669858553	1.9746
80	0.00360947268	0.00326143223	0.00670366419	1.9937
160	0.00094540786	0.00080017118	0.00167768226	1.9985
320	0.00024154741	0.00019803770	0.00041952585	1.9996

Table 4: FVEG-N1 scheme, T=0.1, CFL=0.5

N	$\|\phi(T)-\phi^n\|$	$\|u(T)-u^n\|$	$\|\mathbf{U}(T)-\mathbf{U}^n\|$	EOC
20	0.17589540963	0.06529837724	0.20911917497	
40	0.04832075618	0.01308638944	0.05337280435	1.9701
80	0.01247555949	0.00283409813	0.01340656261	1.9932
160	0.00315867513	0.00065347754	0.00335534309	1.9984
320	0.00079405157	0.00015651727	0.00083905355	1.9996

Table 5: FVEG-N1 scheme, T=0.2, CFL=0.5

N	$\|\phi(T)-\phi^n\|$	$\|u(T)-u^n\|$	$\|\mathbf{U}(T)-\mathbf{U}^n\|$	EOC
20	0.55892402464	0.11225699162	0.59177779767	
40	0.28602634464	0.05665197288	0.30238949704	0.9686
80	0.14568931489	0.02860078232	0.15388109280	0.9746
160	0.07365113809	0.01439264027	0.07775560702	0.9848
320	0.03704518272	0.00722271923	0.03910049337	0.9918

Table 6: FVEG-N2 scheme, T=0.1, CFL=0.5

Example 7.3

In this experiment we apply the first order FVEG3 scheme and the second order FVEG-N1 scheme to the wave equation system combined with the discontinuous initial data

$$\begin{aligned} \phi(x,y,z,0) &= \begin{cases} 1, & x>0 \\ -1, & x<0 \end{cases}, \\ u(x,y,z,0) &= 1.0, \\ v(x,y,z,0) &= w(x,y,z,0)=0. \end{aligned}$$

In Figure 8 we plot $\phi(x,0.5,0.5,0.2)$ restricted to a horizontal line for $80\times80\times80$ mesh. We plot the exact solution as well. It is clear that the FVEG3 scheme smeared the discontinuity, cf. Figure 8 (left). Note that it is a first-order scheme. On the other hand, the second-order FVEG-N1 scheme resolves the discontinuity much better, cf. Figure 8 (right). The oscillations in the solution found by the FVEG-N1 scheme are expected since we have used here no limiter. In the Table 7 we present the CPU costs required for the second order FVEG-N1 scheme on meshes with $N\times N\times N$ cells. These are reasonable computational costs for second order three-dimensional computations. The results were obtained using a personal computer with 3,2 GHz Pentium Processor and 4 GB RAM. Moreover, it should be pointed out that the CPU time of the second FVEG-N1 is actually comparable with that of the first order FVEG schemes.

We conjecture that the superconvergence phenomenon of the N1 method is due to the fact that the source term $\tilde{\mathbf{s}}$, cf. (4.7), that we have neglected, is actually at least of the order $O(\Delta t^3)$. Moreover, it is important to keep the term $\left(\frac{d-1}{d}\right)\mathbf{u}'(P')$ in (7.1), which apparently increases the order of accuracy. The proof of this fact is still open.

N	CPU costs
20	0.14 sec.
40	2.64 sec.
80	37.42 sec.
160	10 min.
320	163 min.

Table 7: Computational time for the FVEG-N1 scheme, T=0.2, CFL=0.5

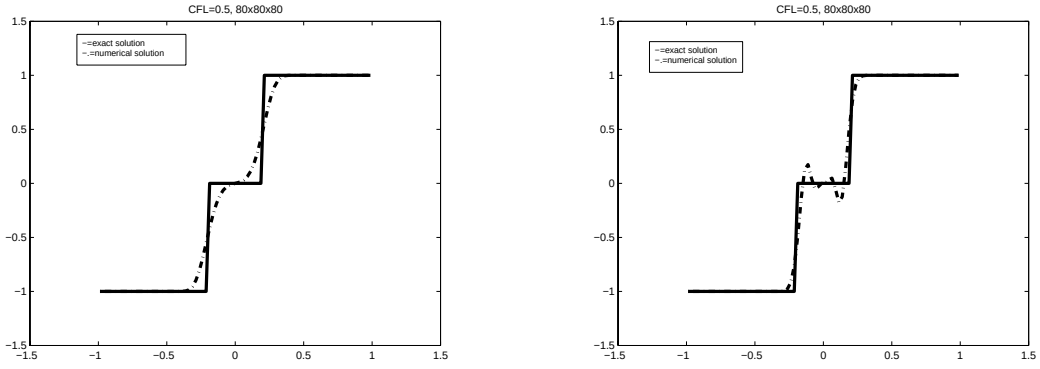

Figure 8: The component $\phi(x, 0.5, 0.5, 0.2)$ of the solution of the wave equation system computed with FVEG3 scheme (left) and FVEG-N1 scheme (right) using $80 \times 80 \times 80$ mesh cells.

8 Conclusions

In this paper we have demonstrated extensibility of the FVEG schemes for three-dimensional systems of hyperbolic conservation laws. It has been shown that the bicharacteristic theory is applicable in order to construct fully three-dimensional numerical schemes based on the finite volume framework. We have illustrated the methodology on a linear system of wave equation. Using the theory of bicharacteristics for three-dimensional linear (or linearized) hyperbolic systems the exact integral equations have been derived. Afterwards using rectangle rule for time integrations and some further manipulations, cf. Lemmas 4.5-4.18 as well as Section 7, the approximate evolution operators for first and second order schemes have been derived. They are multidimensional representations of time evolution of solution, which are explicit in time. Space integrals along the sonic ball, i.e. the base of the bicharacteristic cone for three-dimensional problems, are evaluated exactly for piecewise constant data. The FVEG scheme combines the finite volume update with approximate evolution operators. The time integrals in the finite volume update are approximated by the midpoint rule, space integrations along the cell interfaces are approximated by the trapezoidal rule. Using the approximate operator (7.1) the second order FVEG-N1 scheme has been constructed. Numerical experiments demonstrate the second order EOC.

The main idea of the FVEG schemes is the combination of the finite volume update and multidimensional evolution along the bicharacteristics. The behaviour of new three-dimensional

FVEG schemes has been tested extensively on a series of numerical tests; the representative choice of them is being presented in the paper. The numerical results confirm genuine multidimensional behaviour and discrete vorticity preservation. The methodology presented in the paper for the linear system of the wave equation will be generalized for fully nonlinear problems, e.g. the Euler equations of gas dynamics. This is the goal of our future study.

Acknowledgements.
This research was supported by the VolkswagenStiftung Agency, by the Deutsche Forschungsgemeinschaft Grant No. Wa 633/6-2 as well as and by the Graduate College 413 of the University Hamburg and TU Hamburg-Harburg. Authors gratefully acknowledge these supports.

References

[1] R. Abgrall, M. Mezine. Construction of second order accurate monotone and stable residual distribution schemes for unsteady flow problems. *J. Comput. Phys.* 188(1):16-55, 2003.

[2] S. Billet, E.F. Toro. On WAF-type schemes for multidimensional hyperbolic conservation laws. *J. Comput. Phys.*, 130:1-24, 1997.

[3] D.S. Butler. The numerical solution of hyperbolic systems of partial differential equations in three independent variables. *Proc. Roy. Soc.*, 225A:233–252, 1960.

[4] A. Csk, M. Ricchiuto, H. Deconinck. A conservative formulation of the multidimensional upwind residual distribution schemes for general nonlinear conservation laws. *J. Comput. Phys.*, 179(1):286-312, 2002.

[5] H. Deconinck, P. Roe, R. Struijs. A multidimensional generalization of Roe's flux difference splitter for the Euler equations. *Comput. Fluids*, **22**(2-3):215-222, 1993.

[6] L. C. Evans. *Partial Differential Equations.* American Mathematical Society, 1998.

[7] M. Feistauer, J. Felcman, I. Straškraba. *Mathematical and computational methods for compressible flow.* Oxford University Press, 2003.

[8] M. Fey Multidimensional upwinding, Part II. Decomposition of the Euler equations into advection equations. *J. Comp. Phys.*, 143:181-199, 1998.

[9] T. Kröger, M. Lukáčová-Medviďová. An evolution Galerkin scheme for the shallow water magnetohydrodynamic (SMHD) equations in two space dimensions. *J. Comp. Phys.*, 206:122-149, 2005.

[10] P. Lin, K.W. Morton and E. Süli. Characteristic Galerkin schemes for scalar conservation laws in two and three space dimensions. *SIAM J. Numer. Anal.*, 34(2):779–796, 1997.

[11] P. Lin, K.W. Morton and E. Süli. Euler characteristic Galerkin scheme with recovery. M^2AN, 27(7):863–894, 1993.

[12] R.J. LeVeque. Wave propagation algorithms for multi-dimensional hyperbolic systems. *J. Comp. Phys.*, 131:327-353, 1997.

[13] M. Lukáčová-Medviďová, K. W. Morton and G. Warnecke. Finite volume evolution Galerkin methods for Euler equations of gas dynamics. *Int. J. Num. Methods in Fluids*, 40(3-4):425–434, 2002.

[14] M. Lukáčová-Medviďová, K. W. Morton and G. Warnecke. Finite volume evolution Galerkin FVEG methods for hyperbolic systems. *SIAM J. Sci. Comp.*, 26(1):1–30, 2004.

[15] M. Lukáčová-Medviďová, K.W. Morton and G. Warnecke. High resolution finite volume evolution Galerkin schemes for multidimensional conservation laws. Proceedings of ENUMATH'99, World Scientific Publishing Company, Singapore, 1999.

[16] M. Lukáčová-Medviďová, K.W. Morton and G. Warnecke. Evolution Galerkin methods for hyperbolic systems in two space dimensions. *Math. Comput.*, 69(232):1355–1384, 2000.

[17] M. Lukáčová-Medviďová, K.W. Morton, and G. Warnecke. Evolution Galerkin methods for multidimensional hyperbolic systems. Proceedings of ECCOMAS 2000, Barcelona, 1-14, 2000.

[18] M. Lukáčová-Medviďová, J. Saibertová and G. Warnecke. Finite volume evolution Galerkin methods for nonlinear hyperbolic systems. *J. Comput. Phys.*, 183:533–562, 2002.

[19] M. Lukáčová-Medviďová, J. Saibertová, G. Warnecke and Y. Zahaykah. On evolution Galerkin methods for the Maxwell and the linearized Euler equations. *Appl. Math.*, 49(5):415–439, 2004.

[20] M. Lukáčová-Medviďová, Z. Vlk. Well-balanced finite volume evolution Galerkin methods for the shallow water equations with source terms, *Int. J. Num. Fluids* 47(10-11):1165-1171, 2005.

[21] M. Lukáčová-Medviďová, G. Warnecke, and Y. Zahaykah. Third order finite volume evolution Galerkin (FVEG) methods for two-dimensional wave equation system. *J. Numer. Math.*, 11(3):235–251, 2003.

[22] M. Lukáčová-Medviďová, G. Warnecke and Y. Zahaykah. On the stability of the evolution Galerkin schemes applied to a two-dimensional wave equation system. *in print SIAM J. Numer. Anal.*, 2004.

[23] S. Noelle. The MOT-ICE: a new high-resolution wave-propagation algorithm for multidimensional systems of conservative laws based on Fey's method of transport. *J. Comput. Phys.*, 164:283-334, 2000.

[24] S. Ostkamp. Multidimensional characteristic Galerkin schemes and evolution operators for hyperbolic systems. *Math. Meth. Appl. Sci.*, 20:1111–1125, 1997.

[25] P. Prasad and R. Ravindran. Canonical form of a quasilinear hyperbolic system of first order equations. *J. Math. Phys. Sci.*, 18(4):361–364, 1984.

[26] A.S. Reddy, V.G. Tikekar, and P. Prasad. Numerical solution of hyperbolic equations by method of bicharacteristics. *J. Math. Phys. Sci.*, 16(6):575–603, 1982.

[27] Qurrat-ul-Ain. *Multidimensional Schemes for Hyperbolic Conservation Laws on Triangular Meshes*. Dissertation, University of Magdeburg, 2005.

[28] Qurrat-ul-Ain, G. Warnecke and Y. Zahaykah: On the finite volume evolution Galerkin (FVEG) methods for two-dimensional first order hyperbolic systems on structured and unstructured triangular meshes, *in preperation*.

[29] Y. Zahaykah. *Evolution Galerkin Schemes and Discrete Boundary Conditions for Multidimensional First Order Systems*. Dissertation, Magdeburg, 2002.